PHYSICAL REVIEW D **83,** 104050 (2011)

Electric charge on the brane?

Burkhard Kleihaus,[1] Jutta Kunz,[1] Eugen Radu,[2,3] and Daniel Senkbeil[1]

[1]*Institut für Physik, Universität Oldenburg, Postfach 2503 D-26111 Oldenburg, Germany*
[2]*School of Theoretical Physics—DIAS, 10 Burlington Road, Dublin 4, Ireland*
[3]*Department of Computer Science, National University of Ireland Maynooth, Maynooth, Ireland*

(Received 30 March 2011; published 27 May 2011)

We consider black holes localized on the brane in the Randall-Sundrum infinite braneworld model. These configurations are static and charged with respect to a spherically symmetric, electric Maxwell field living on the brane. We start by attempting to construct vacuum black holes, in which case our conclusions are in agreement with those of Yoshino [J. High Energy Phys. 01 (2009) 068]. Although approximate solutions appear to exist for sufficiently small brane tension, these are likely only numerical artifacts. The qualitative features of the configurations in the presence of a brane U(1) electric field are similar to those in the vacuum case. In particular, we find a systematic unnatural behavior of the metric functions in the asymptotic region in the vicinity of the anti–de Sitter horizon. Our results are most naturally interpreted as evidence for the nonexistence of static, nonextremal charged black holes on the brane. In contrast, extremal black holes are more likely to exist on the brane. We determine their near-horizon form by employing both analytical and numerical methods. For any bulk dimension $d > 4$, we find good agreement between the properties of large extremal black holes and the predictions of general relativity, with calculable subleading corrections.

DOI: 10.1103/PhysRevD.83.104050 PACS numbers: 04.70.Dy, 04.50.Cd, 04.50.Gh

I. INTRODUCTION

The Randall-Sundrum (RS) infinite braneworld scenario [1] has been proposed as a mechanism to explain the hierarchy between the TeV scale and the Planck scale, and to realize four-dimensional gravity effectively on the 3-brane. In this model, the observable universe is a 3-brane (domain wall) to which standard model fields are confined, while gravity can access the extra spatial dimensions. The bulk metric is a locally anti–de Sitter (AdS) spacetime satisfying the Einstein equations with negative cosmological constant. At low enough energy, perturbative Newtonian gravity is recovered on the brane at distances large compared to the AdS length scale ℓ.

The existence of black hole solutions in the RS model is an interesting open problem (see, e.g., Kanti [2] for a recent review on this issue). *A priori*, it is not clear why such black hole solutions should not exist, and the existence of bulk black hole solutions would imply that there are also black hole solutions on the brane. Indeed, such exact black hole solutions were found by Emparan *et al.* [3] for the dimension $d = 4$ of the bulk spacetime, where the static black hole is localized on a 2-brane. The construction of such black hole solutions in [3] relied on the existence of a special class of solutions of the $d = 4$ Einstein gravity—the so-called C metric [4], and the brane is a suitable slice in this spacetime.

However, in the absence of a $d > 4$ generalization of the C metric, the existence of higher dimensional brane world black holes is controversial. Although Dadhich *et al.* [5] proposed an analytic solution for brane black holes in the $d = 5$ RS scenario, this result was obtained subject to approximations whose validity is not clear. In that approach, the braneworld Einstein equations [6] were solved assuming a particular form for the bulk Weyl tensor on the wall. Interestingly, this resulted in a Reissner-Nordström (RN) geometry, although there is no brane electric charge. However, in this case only the induced metric on the brane was found, without solving the bulk equations of motion. Thus the solution proposed in [5] for a brane black hole in the RS scenario is not really satisfactory.

Hence, for bulk dimensions $d > 4$, one has to rely on numerical methods to address the existence of black holes in the RS model. So far, the only results supporting the existence of such solutions on a nonperturbative level are those by Kudoh *et al.* [7,8]. They were obtained within an in principle rigorous approach, i.e., by solving the full set of equations in the bulk with suitable boundary conditions on the brane. Reporting numerical results for spacetime dimensions $d = 5$ and 6, Kudoh *et al.* [7,8] presented localized black holes whose horizon radius was much smaller than the AdS length scale. In contrast, for larger black holes their numerical accuracy decreased and convergence was lost within their numerical scheme.

Moreover, the recent numerical work of Yoshino [9] (while finding agreement with earlier perturbative [10] and numerical [7,8] results) also failed to find such large black hole configurations. Performing a careful error analysis in terms of systematic and nonsystematic errors, Yoshino [9] concluded that the positive results in [7,8] were nothing but numerical artifacts, mainly due to an inappropriate treatment of the outer boundary of the integration region.

In fact, Emparan *et al.* [11] and also Tanaka [12] had earlier put forward a number of theoretical arguments against the existence of $d > 4$ *static* black holes on the brane in the RS model, which were mainly based on a version of the AdS/CFT correspondence. According to the conjecture by Emparan *et al.* [11], such bulk black holes would necessarily be time dependent, since their duals would describe quantum corrected black holes in a $d-1$ dimensional braneworld. Counterarguments were, however, given by Fitzpatrick *et al.* [13]. Further results on black holes localized on the brane can be found in [14–17].

Motivated by these conflicting arguments and results, we have performed an independent investigation of the issue of the numerical construction of $d > 4$ braneworld black holes. Similar to the previous work by Kudoh *et al.* [7,8] and Yoshino [9], we have solved the bulk Einstein equations with Israel junction conditions on the brane, employing different numerical methods from those in [7–9]. In particular, we have used a compactified radial coordinate which in principle avoids the problems associated with the position of the outer boundary of integration for the radial coordinate.

The results we have found for bulk dimensions $d = 5$ and 6 support the claim of Yoshino [9] that "a solution sequence of a static black hole on an asymptotically flat brane that is reduced to the Schwarzschild black hole in the zero tension limit is unlikely to exist." In particular, we have noticed a systematic unnatural behavior of the metric functions for large values of the radial coordinate, i.e. close to the AdS horizon. This behavior seems to be at the origin of the loss of numerical convergence for large black holes.

Obviously, it is interesting to examine how generic this behavior is, and whether it can be circumvented in more general cases. Perhaps the simplest more general case to be studied corresponds to black hole solutions, which are *electrically* charged with respect to a Maxwell field living on the brane. This type of solution was considered by Chamblin *et al.* [18], following a different approach, however. There the "initial" data on the brane was prescribed, and then it was evolved in the spacelike direction transverse to the brane, by solving the bulk equations numerically. The results in [18] show the occurrence of pathological features in the bulk for any initial data. However, Chamblin *et al.* [18] postulated a special restricted form of the braneworld metric, with a single essential function; moreover, the numerical integration employed a relatively small cutoff radius.

Our present approach is rather different from [18], since we attempt to directly solve the bulk vacuum Einstein equations with suitable boundary conditions. The bulk theory is the same as for the uncharged case, the electric charge entering the problem via the Israel junction conditions on the brane. Restricting to static, nonextremal configurations in an AdS_5 bulk, our results show that all pathologies present for vacuum black holes occur also in this case. Therefore, we conclude that the existence of static, charged, nonextremal solutions is unlikely, as well.

Turning next to static, extremal, electrically charged black holes in the RS braneworld scenario, however, we anticipate that such solutions are more likely to exist, since a number of arguments put forward against the existence of static black holes do not apply when the Hawking temperature vanishes. Here we investigate the near-horizon structure of extremal black hole solutions with electric charge on the brane, without attempting to construct the full configurations. This restriction leads to a system of coupled nonlinear ordinary differential equations, which are solved numerically within a nonperturbative approach for several dimensions $d \geq 5$ of the bulk.

For a five-dimensional AdS bulk, this problem has been considered by Kaus and Reall [19]. In this work we generalize their results for any $d \geq 5$ dimensions, and show that for large black holes, there is good agreement for the induced metric on the brane and for the entropy with the predictions of general relativity (GR), with calculable subleading corrections.

The paper is organized as follows: in the next section we present our results for nonextremal black holes in the RS braneworld model, employing a nonperturbative approach, by directly solving a set of three nonlinear partial differential equations with suitable boundary conditions. In Sec. III we consider extremal black holes that are charged with respect to a purely electric Maxwell field on the brane and determine their near-horizon form. We give our conclusions and remarks in the final section. The Appendix contains a discussion of some technical aspects involved in our numerical investigation of nonextremal braneworld black holes.

II. NONEXTREMAL CONFIGURATIONS

A. The problem

We consider the RS braneworld model, with a d-dimensional bulk spacetime and a single $(d-1)$-dimensional brane with positive tension in it. Also, we impose Z_2 symmetry about the brane, which is assumed to be asymptotically flat. The bulk matter is merely a negative cosmological constant, and the brane tension and the matter localized on the brane are treated in a distributional sense.

The action of this model is

$$S = \frac{1}{16\pi G_d}\int_{\mathcal{M}} d^d x\sqrt{-g}(R-2\Lambda) + \int_{\text{brane}} d^{d-1}x\sqrt{-h}\left(\frac{1}{8\pi G_d}K - \sigma - \frac{1}{16\pi G_{d-1}}F_{\mu\nu}F^{\mu\nu}\right), \tag{2.1}$$

where $\mathcal{M}$ is the bulk spacetime, $\Lambda = -(d-2)/(d-1)/(2\ell^2)$ is the bulk cosmological constant, and $K_{\mu\nu}$ is the projection of the extrinsic curvature of the brane

hypersurface with induced metric $h_{\mu\nu}$. Also G_d is Newton's constant in d-spacetime dimensions; σ and $F = dA$ are the brane tension and the field strength of the Maxwell field on the brane, respectively.

From the above action, we obtain the d-dimensional Einstein equation in the bulk

$$R_{ij} - \tfrac{1}{2}Rg_{ij} + \Lambda g_{ij} = 0. \tag{2.2}$$

For the RS infinite braneworld scenario, the Israel junction conditions on the brane are given by [20]

$$K_{\mu\nu} - Kh_{\mu\nu} = 4\pi G_d\left(-\sigma h_{\mu\nu} + \frac{1}{4\pi G_{d-1}}t_{\mu\nu}\right), \tag{2.3}$$

where $t_{\mu\nu}$ is the energy-momentum tensor of the matter fields on the brane. For a U(1) field, the expression of $t_{\mu\nu}$ is

$$t_{\mu\nu} = F_{\mu\alpha}F_{\nu}{}^{\alpha} - \tfrac{1}{4}F_{\alpha\beta}F^{\alpha\beta}h_{\mu\nu}. \tag{2.4}$$

We shall set the brane tension to the RS value

$$\sigma = \frac{1}{4\pi G_d}\frac{d-2}{\ell},$$

while

$$G_{d-1} = \frac{d-3}{2\ell}G_d.$$

This simplifies Eq. (2.3) to

$$K_{\mu\nu} - Kh_{\mu\nu} = -\frac{d-2}{\ell}h_{\mu\nu} + \frac{2\ell}{d-3}t_{\mu\nu}, \tag{2.5}$$

which is the form used in what follows. The brane U(1) field is a solution of the Maxwell equations

$$\nabla_\mu F^{\mu\nu} = 0, \tag{2.6}$$

for a metric background given by $h_{\mu\nu}$.

1. The ansatz and the equations

The metric ansatz employed here essentially corresponds to the one used in the previous studies [7–9]. The black hole metric is spherically symmetric on the brane and axisymmetric in the bulk spacetime, with line element

$$ds^2 = \frac{1}{z^2(r,\chi)}\left(e^{2B(r,\chi)}\left(\frac{dr^2}{F(r)} + r^2d\chi^2\right) + e^{2C(r,\chi)}r^2\sin^2\chi d\Omega_{d-3}^2 - e^{2A(r,\chi)}F(r)dt^2\right), \tag{2.7}$$

which is parametrized in terms of two background functions

$$F(r) = 1 - \left(\frac{r_0}{r}\right)^{d-3}, \qquad z(r,\chi) = 1 + \frac{r}{\ell}\cos\chi, \tag{2.8}$$

and three unknown metric functions $A(r,\chi)$, $B(r,\chi)$, and $C(r,\chi)$. In the above relations, r_0 is a positive constant and $d\Omega_{d-3}^2$ is the metric on the $(d-3)$ sphere. The background functions $F(r)$ and $z(r,\chi)$ have been introduced such that two important limits of the general solution are already contained within the ansatz (2.7). For $\ell \to \infty$ one finds the well-known Schwarzschild-Tangherlini black hole, expressed in the usual Schwarzschild coordinates.[1] Another limit of interest is $r_0 = 0$, in which case one recovers the original RS model, i.e. a part of AdS_d spacetime expressed in Poincaré coordinates (and $A = B = C = 0$ in both limits).

The event horizon is supposed to reside at a surface of constant radial coordinate $r = r_0$ and characterized by the condition $F(r_0) = 0$, while the brane is located at $\chi = \pi/2$. Then the coordinate range considered is $r_0 \le r < \infty$ and $0 \le \chi \le \pi/2$. Therefore the coordinates in Eq. (2.7) have a rectangular boundary and thus are suitable for the numerical methods employed.

The induced metric on the brane has line element[2]

$$d\sigma^2 = g_{rr}(r)dr^2 + g_{\Omega\Omega}(r)d\Omega_{d-3}^2 + g_{tt}(r)dt^2, \tag{2.9}$$

with

$$g_{rr}(r) = \frac{e^{2B(r,\pi/2)}}{F(r)}, \qquad g_{\Omega\Omega}(r) = e^{2C(r,\pi/2)}r^2, \qquad g_{tt}(r) = -e^{2A(r,\pi/2)}F(r), \tag{2.10}$$

i.e. it describes a static, spherically symmetric black hole spacetime in $d-1$ dimensions.

The equations satisfied by the functions A, B, and C are found by using a suitable combination of the Einstein equations, $G_t^t + \Lambda = 0$, $G_r^r + G_\chi^\chi + 2\Lambda = 0$, and $G_\phi^\phi + \Lambda = 0$ (where ϕ denotes an angle of the $d-3$-dimensional sphere) and read[3]

[1] References [7–9] preferred to describe the Schwarzschild black hole in isotropic coordinates, which was also our initial choice. However, we realized that a Schwarzschild coordinate system together with the coordinate transformation (2.16) improved the quality of the numerical calculations for $d = 5$.

[2] Note the presence of three distinct metric functions in Eq. (2.9). In contrast, in GR only two metric functions are present, with the usual choices $g_{rr} = 1/N(r)$, $g_{\Omega\Omega} = r^2$, and $g_{tt} = N(r)\sigma^2(r)$.

[3] One can see that the case $d = 4$ is special, since a number of terms vanish in this case. However, the structure of the equations is the same for any $d > 4$.

$$A'' + \frac{1}{r^2 F}\ddot{A} + \left(\frac{d-2}{r} + \frac{3F'}{2F}\right)\left(A' - \frac{\cos\chi}{\ell z}\right) + \frac{(d-3)F'}{2F}\left(C' - \frac{\cos\chi}{\ell z}\right) + \left(A' - \frac{\cos\chi}{\ell z}\right)^2 + (d-3)\left(A' - \frac{\cos\chi}{\ell z}\right)\left(C' - \frac{\cos\chi}{\ell z}\right)$$
$$+ \frac{(d-3)\cot\chi}{r^2 F}\left(\dot{A} + \frac{r\sin\chi}{\ell z}\right) + \frac{1}{r^2 F}\left(\dot{A} + \frac{r\sin\chi}{\ell z}\right)^2 + \frac{(d-3)}{r^2 F}\left(\dot{A} + \frac{r\sin\chi}{\ell z}\right)\left(\dot{C} + \frac{r\sin\chi}{\ell z}\right) - \frac{(d-1)e^{2B}}{\ell^2 F z^2}$$
$$+ \frac{1}{rF}\frac{(r + \ell\cos\chi)}{\ell^2 z^2} + \frac{\cos^2\chi}{\ell^2 z^2} = 0, \tag{2.11}$$

$$B'' + \frac{1}{r^2 F}\ddot{B} - \frac{(d-3)}{r}\left(A' - \frac{\cos\chi}{\ell z} + (d-4)\left(C' - \frac{\cos\chi}{\ell z}\right)\right) + \frac{1}{r}\left(B' - \frac{\cos\chi}{\ell z}\right) + \frac{F'}{2F}\left(B' - \frac{\cos\chi}{\ell z}\right) - \frac{(d-3)F'}{2F}\left(C' - \frac{\cos\chi}{\ell z}\right)$$
$$- (d-3)\left(A' - \frac{\cos\chi}{\ell z}\right)\left(C' - \frac{\cos\chi}{\ell z}\right) - \frac{1}{2}(d-3)(d-4)\left(C' - \frac{\cos\chi}{\ell z}\right)^2 - (d-3)\frac{\cot\chi}{r^2 F}\left(\dot{A} + \frac{r\sin\chi}{\ell z} + (d-4)\left(\dot{C} + \frac{r\sin\chi}{\ell z}\right)\right)$$
$$- \frac{(d-3)}{r^2 F}\left(\dot{A} + \frac{r\sin\chi}{\ell z}\right)\left(\dot{C} + \frac{r\sin\chi}{\ell z}\right) - \frac{(d-3)(d-4)}{2r^2 F}\left(\dot{C} + \frac{r\sin\chi}{\ell z}\right)^2 + (d-3)(d-4)\frac{e^{2(B-C)}}{2\sin^2\chi F r^2} + \frac{(d-1)(d-4)e^{2B}}{2\ell^2 F z^2}$$
$$- \frac{(d-3)(d-4)}{2r^2}\left(1 + \frac{\cot^2\chi}{F}\right) - \frac{(d-4)F'}{2rF} + \frac{1}{\ell^2 z^2}\left(\cos^2\chi + \frac{r + \ell\cos\chi}{rF}\right) = 0, \tag{2.12}$$

$$C'' + \frac{1}{r^2 F}\ddot{C} + (d-3)\left(C' - \frac{\cos\chi}{\ell z}\right)^2 + \frac{1}{r}\left(A' - \frac{\cos\chi}{\ell z}\right) + \frac{2d-5}{r}\left(C' - \frac{\cos\chi}{\ell z}\right) + \frac{F'}{F}\left(C' - \frac{\cos\chi}{\ell z}\right) + \left(A' - \frac{\cos\chi}{\ell z}\right)\left(C' - \frac{\cos\chi}{\ell z}\right)$$
$$+ \frac{(d-3)}{r^2 F}\left(\dot{C} + \frac{r\sin\chi}{\ell z}\right)^2 + \frac{\cot\chi}{r^2 F}\left(\dot{A} + \frac{r\sin\chi}{\ell z}\right) + \frac{2(d-3)\cot\chi}{r^2 F}\left(\dot{C} + \frac{r\sin\chi}{\ell z}\right) + \frac{1}{r^2 F}\left(\dot{A} + \frac{r\sin\chi}{\ell z}\right)\left(\dot{C} + \frac{r\sin\chi}{\ell z}\right)$$
$$- (d-4)\frac{e^{2(B-C)}}{r^2 F\sin^2\chi} - (d-1)\frac{e^{2B}}{\ell^2 F z^2} + \frac{r + \ell\cos\chi}{F\ell^2 r z^2} + \frac{d-3}{r^2} + \frac{\cos^2\chi}{\ell^2 z^2} + \frac{1}{r^2 F}((d-4)\cot^2\chi - 1) + \frac{F'}{rF} = 0, \tag{2.13}$$

where a prime denotes the derivative with respect to the radial variable r and a dot denotes the derivative with respect to the angular variable χ. The remaining equations $G^r_\chi = 0$, $G^r_r - G^\chi_\chi = 0$ yield two constraints. Following [21], we note that setting $G^t_t + \Lambda = 0$, $G^r_r + G^\chi_\chi + 2\Lambda = 0$, $G^\phi_\phi + \Lambda = 0$ in $\nabla_\mu G^{\mu r} = 0$ and $\nabla_\mu G^{\mu\chi} = 0$, we obtain Cauchy-Riemann relations for G^r_χ and $G^r_r - G^\chi_\chi$. Thus the weighted constraints satisfy Laplace equations, and the constraints are fulfilled, when one of them is satisfied on the boundary and the other at a single point [21].

For completeness, we here present also the expressions for the Hawking temperature T_H and the event horizon area $A^{(d)}_H$ of a bulk black hole,

$$T_H = e^{A(0,\chi) - B(0,\chi)}\frac{(d-3)}{4\pi r_0},$$
$$A^{(d)}_H = V_{d-3} r_0^{d-2}\int_0^{\pi/2} e^{B(0,\chi) + (d-3)C(0,\chi)}\frac{\sin^{d-3}\chi}{(1 + \frac{r_0}{\ell}\cos\chi)^{d-2}}d\chi, \tag{2.14}$$

where V_{d-3} is the area of the unit S^{d-3} sphere. (The Einstein equation $G^r_\chi = 0$ implies that e^{A-B} is indeed constant on the horizon.) The associated black hole on the brane would have the same Hawking temperature as the bulk solution, while its event horizon area would be

$$A^{(d-1)}_H = V_{d-3} r_0^{d-3} e^{(d-3)C(0,\pi/2)}. \tag{2.15}$$

In practice, we have found it convenient to introduce the radial coordinate[4]

$$\rho = \sqrt{r^2 - r_0^2}, \tag{2.16}$$

such that the horizon would reside at $\rho = 0$, which gives a simpler set of boundary conditions for the black hole horizon. The transformation then results in a new form of the general ansatz (2.7) with

$$ds^2 = \frac{1}{z^2(\rho,\chi)}\left(e^{2B(\rho,\chi)}\left(\frac{d\rho^2}{F_1(\rho)} + (\rho^2 + r_0^2)d\chi^2\right) + e^{2C(\rho,\chi)}(\rho^2 + r_0^2)\sin^2\chi d\Omega^2_{d-3} - e^{2A(\rho,\chi)}F_2(\rho)dt^2\right), \tag{2.17}$$

where $F_1(\rho) = F(r(\rho))(\rho^2 + r_0^2)/\rho^2$ and $F_2(\rho) = F(r(\rho))$. [Note that $F_1(\rho) \to (d-3)/2 + O(\rho^2)$, $F_2(\rho) \to (d-3)\rho^2/(r_0^2) + O(\rho^4)$ as $\rho \to 0$.] The temperature and the horizon area are still given by (2.14) and (2.15).

[4]This change of the radial coordinate proved useful before in the numerical study of nonuniform black string solutions [22], which is an axisymmetric problem with some similarities to the problem studied here.

2. U(1) field on the brane and boundary conditions

Perhaps the simplest example of nonvacuum solutions in the RS infinite braneworld scenario is provided by a Maxwell field confined to the brane. In this work we shall restrict to a static, spherically symmetric, purely electric field with U(1) potential

$$A = V(\rho)dt. \tag{2.18}$$

Thus the field strength tensor is $F = \frac{dV}{d\rho} d\rho \wedge dt$. The Maxwell equations (2.6) imply the existence of the first integral

$$V(\rho) = Q \int d\rho \frac{\rho}{(\rho^2 + r_0^2)^{(d-2)/2}} \times e^{A(\rho,\pi/2)+B(\rho,\pi/2)-(d-3)C(\rho,\pi/2)}, \tag{2.19}$$

where Q is an integration constant that fixes the electric charge on the brane.

The numerical solution of the equations is pursued subject to the following set of boundary conditions:

$$\partial_\rho A|_{\rho=0} = \partial_\rho B|_{\rho=0} = \partial_\rho C|_{\rho=0} = 0, \tag{2.20}$$

on the black hole horizon,

$$A|_{\rho=\infty} = B|_{\rho=\infty} = C|_{\rho=\infty} = 0, \tag{2.21}$$

at infinity, and

$$\partial_\chi A|_{\chi=0} = \partial_\chi B|_{\chi=0} = \partial_\chi C|_{\chi=0} = 0, \tag{2.22}$$

on the symmetry axis. Regularity at $\chi = 0$ further requires that $B|_{\chi=0} = C|_{\chi=0}$. This condition can be implemented by working with the new function $\bar{C} = C - B$. The Israel junction condition (2.5) together with the expression (2.19) for the U(1) potential lead to the following boundary conditions on the brane:

$$\begin{aligned}\partial_\chi A|_{\chi=\pi/2} &= \partial_\chi B|_{\chi=\pi/2} \\ &= \frac{\sqrt{\rho^2 + r_0^2}}{\ell}(e^{B(\rho,\pi/2)} - 1) + \frac{2d-7}{(d-2)(d-3)} \\ &\quad \times e^{B(\rho,\pi/2)-2(d-3)C(\rho,\pi/2)} \frac{\ell}{(\rho^2 + r_0^2)^{(2d-7)/2}} Q^2, \\ \partial_\chi C|_{\chi=\pi/2} &= \frac{\sqrt{\rho^2 + r_0^2}}{\ell}(e^{B(\rho,\pi/2)} - 1) - \frac{3}{(d-2)(d-3)} \\ &\quad \times e^{B(\rho,\pi/2)-2(d-3)C(\rho,\pi/2)} \frac{\ell}{(\rho^2 + r_0^2)^{(2d-7)/2}} Q^2,\end{aligned} \tag{2.23}$$

where $Q = 0$ corresponds to the vacuum limit.

B. Numerical results

The results exhibited in this section concern the physically most interesting case $d = 5$ (i.e. a 3-brane). However, we have observed a similar behavior when considering vacuum black holes for a 4-brane instead.

The numerical calculations have been based on the Newton-Raphson method and been performed with help of the program FIDISOL/CADSOL [23], which also provides an error estimate for each unknown function. Different from previous work on this problem, in our approach the boundary conditions (2.21) are really imposed at $\rho = \infty$. This is achieved by employing a compactified radial coordinate $x = \rho/(1 + \rho)$ which maps $\rho = \infty$ to the finite value $x = 1$. Further details on the numerical method are given in the Appendix.

The first relevant input parameter for our problem is the dimensionless ratio

$$L = \frac{r_0}{\ell}. \tag{2.24}$$

Without any loss of generality, by using a simple rescaling of ρ, one can set r_0 to take a fixed value, and then vary the AdS length scale ℓ. The results reported in this section correspond to the choice $r_0 = 1$, although similar results have been found for other values of r_0. In the charged case, there is a second input parameter of the problem, which is the ratio

$$q = \frac{Q}{r_0^{d-3}}. \tag{2.25}$$

1. The vacuum case ($Q = 0$)

Similar to Kudoh *et al.* [7,8] and Yoshino [9], we have first applied the numerical procedure to the above stated set of equations and boundary conditions, choosing a large value of the AdS length scale ℓ (typically $L \simeq 10^{-4}$–10^{-3}) and employing the initial guess[5] $A = B = C = 0$. In this case, the solver has converged and provided numerical output with good accuracy.[6] The functions A, B, and C have a nontrivial shape, but their magnitude is small, almost zero. Next, we have started a new iteration and employed these data as an initial guess for a slightly larger value of L. Again, the solver has converged and provided apparently reasonable numerical output, which in turn has been used as input for the next iteration for another slightly larger value of L, etc. For all configurations with sufficiently small values of L, we have found good agreement of the extracted physical properties with those reported by Kudoh *et al.* [7,8], obtained within their numerical scheme.

In principle, working in small steps, one expects to find solutions for arbitrarily large values of L in this way. However, for any grid choice employed, we have noticed that the numerical accuracy appeared to be progressively deteriorating with increasing L. Around $L \simeq 0.3$ finally, the

[5]We note that for $L \neq 0$, $A = B = C = 0$ is *not* a solution of the field equations unless $r_0 = 0$.

[6]The computed relative error of the "solution" (truncation error) was on the order of 0.001 in this case.

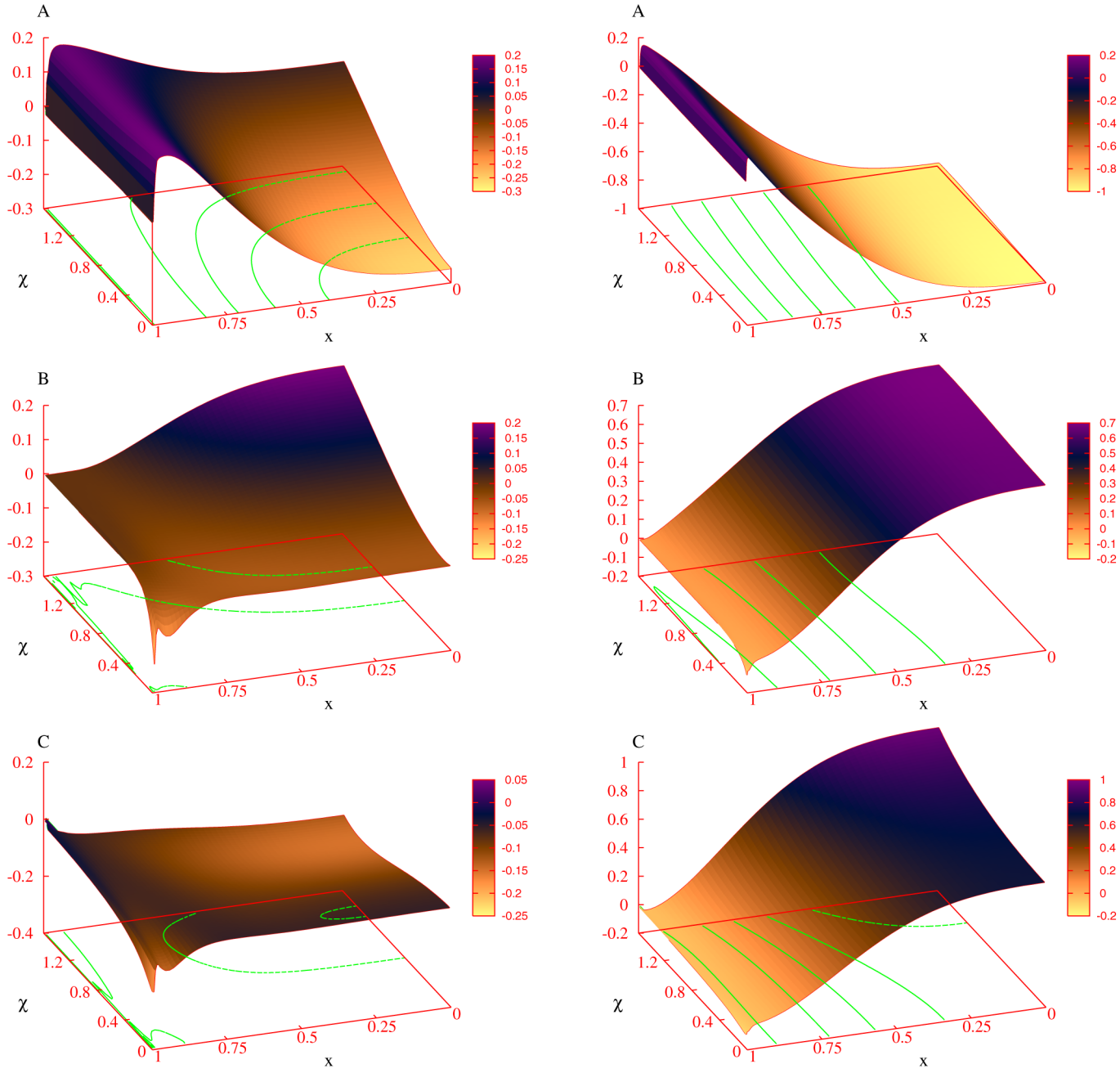

FIG. 1 (color online). The metric functions A, B, and C are shown as functions of the compactified radial coordinate $x = \rho/(1 + \rho)$ and the angular variable χ for a vacuum configuration with $L = 1$ (left panel) and a charged one with $L = 0.24$, $q = 1.73$ (right panel).

numerical errors have turned unacceptably large for the configurations,[7] while for still larger values of L the numerical errors have accumulated further, until finally convergence of the numerical scheme has been lost.

In our scheme, the numerical problems appear to originate mainly in the asymptotic region.[8] As L increases, the metric functions start to develop an increasingly unnatural shape for large values of the radial coordinate (typically for $\rho > 10\ell$) and all values of χ (although in some functions this feature is more pronounced for $\chi \to 0$). This unnatural behavior manifests itself in the occurrence of "oscillations" of the metric functions in the far field.[9] The amplitude of these oscillations increases with increasing L. At the same time these oscillations start at increasingly

[7]This has also been manifest in the constraint equations G^{ρ}_{χ} and $G^{\rho}_{\rho} - G^{\chi}_{\chi}$, implying large errors in the evaluation of a Hawking temperature.

[8]In previous numerical work numerical problems were largely associated with the symmetry axis $\chi = 0$.

[9]A similar behavior was noticed by Yoshino [9] (see his Fig. 3).

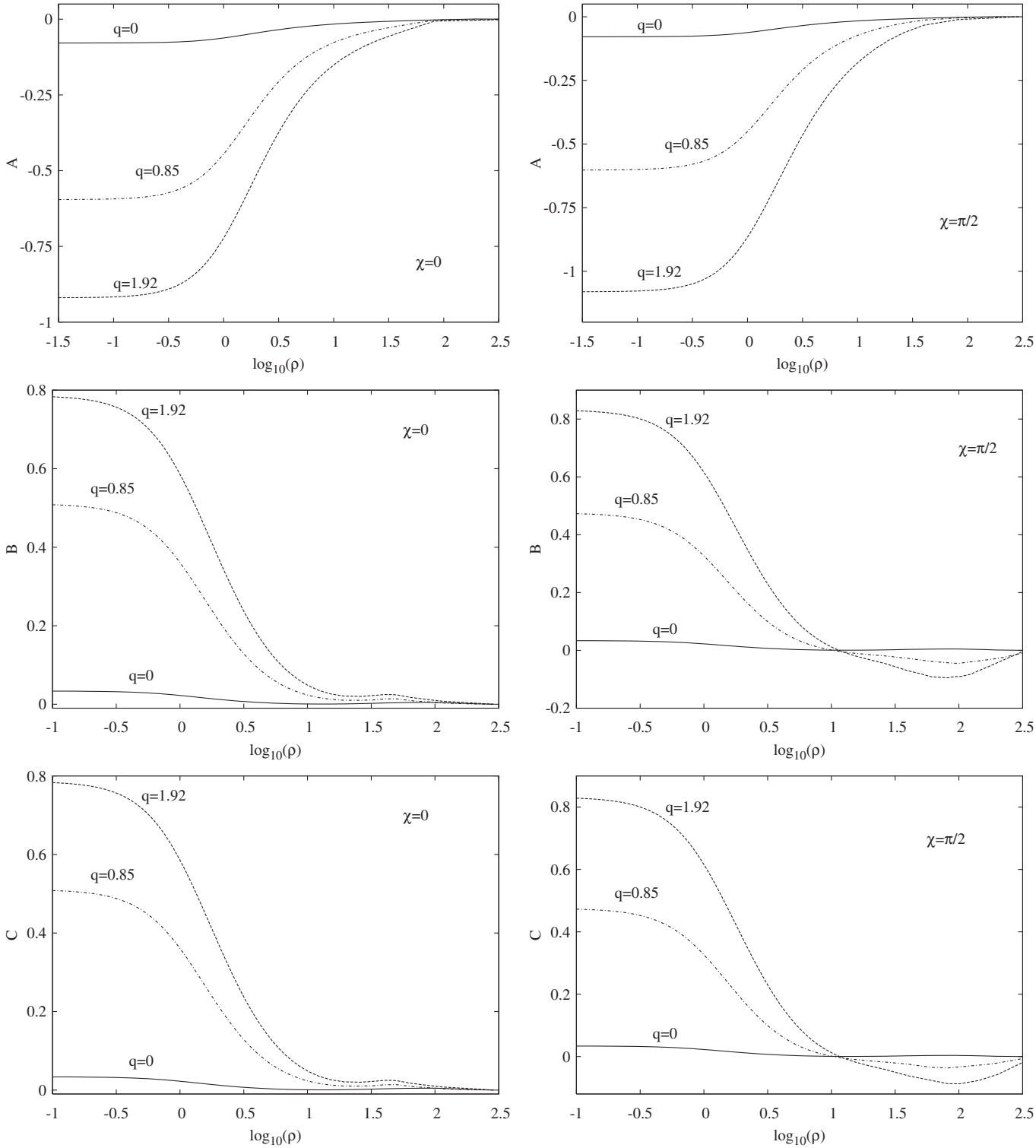

FIG. 2. The metric functions A, B, and C are shown at $\chi = 0$ (on the symmetry axis) and at $\chi = \pi/2$ (on the brane) for configurations for $L = 10$ and three values of the charge parameter q.

smaller values of the radial coordinate. We illustrate this unnatural behavior of the metric functions close to the AdS horizon for a typical $d = 5$ calculation (with large numerical errors) in Fig. 1 (left panels) and also in Fig. 2 (the case with $q = 0$).

This unnatural behavior appears for all grid choices and all metric parametrizations considered, including the ones employed in [7–9]. Also, quite interesting, when working with a finite grid with cutoff radius $\rho_{\max} \simeq 10 r_0$ (the typical case considered in [7]), one usually fails to

detect this oscillatory behavior, since it appears only for larger values of the radial coordinate. (A distinct dependence of the numerical results on the value of $\rho_{\max}$ was already noticed by Yoshino [9], representing an essential part of the nonsystematic error present in his calculations.)

Moreover, since the numerical error increases gradually, it is impossible to identify a critical value L_c, such that one could claim nonexistence of the solutions for $L > L_c$. Thus the oscillations are likely to exist for any value of L. We surmise that for very small values of L such a behavior is located at values of x very close to unity (i.e. at very large values of ρ), and that the amplitude of the oscillations is at the same time very small (and thus difficult to detect within the numerical approach employed).

2. U(1) field on the brane

It is interesting to examine whether the above results hold also for more general cases. In particular, one would like to know whether the unnatural asymptotic behavior, that we have noticed in the vacuum case, survives in the presence of matter fields on the brane or whether it can be circumvented due to their presence.

The simplest case one may think of corresponds to a spherically symmetric static Maxwell field living on the brane. As one can see from Eqs. (2.23), although the bulk equations are the same as in the vacuum case, the presence of the U(1) field leads to a different set of boundary conditions on the brane and thus to a different geometry in the bulk. Naively, one may then expect the metric on the brane to correspond to a RN black hole with corrections.

Our initial hope has been that the presence of an electric charge on the brane would make the numerical scheme more stable. However, in contrast to our expectations, our results for typical charged configurations have turned out to be qualitatively similar to the vacuum case.[10] For a given value of L, we have employed the corresponding vacuum data as the initial guess for the numerical integration of the equations in the presence of a small electric charge Q. Subsequently, we have slowly increased the value of Q, and thus the second dimensionless parameter q.

For small values of L (typically $L < 0.1$), the solver has converged and has provided apparently reasonable numerical output, as in the vacuum case. In particular, the shape of the functions appears to be rather insensitive to the value of q, while their magnitude is increasing with q. When extracting the Hawking temperature and the horizon area from the numerical data for these small values of L, we have observed that for fixed L the Hawking temperature decreases with increasing q as expected, while the horizon area increases for the ''supposed'' bulk black hole as well as for the associated supposed black hole on the brane.

However, for any value of q employed, we have seen the numerical accuracy of the calculations to strongly deteriorate with increasing L as in the vacuum case, until at some stage the numerical solver has stopped to converge. Moreover, the behavior of the metric functions for large values of ρ is also qualitatively similar to what we have found for $q = 0$, while the magnitude of the oscillations in the asymptotic region even increases with increasing q, as seen in Fig. 2. This unnatural behavior appears to be generic for any choice of the nonequidistant grid employed in the integration, and we conclude that all pathologies observed for vacuum configurations are also present in the charged case. Clearly, this puts the existence of such charged black hole solutions into strong doubt.

We would like to emphasize that all of the configurations obtained numerically yield a nonvanishing Hawking temperature and thus would correspond to nonextremal black holes (if they were indeed solutions). Evaluated according to Eq. (2.14), the expression for the Hawking temperature does not yield a strictly constant value, but typically varies slightly (because of the numerical error), as long as L and q are sufficiently small. For the charged configurations obtained here, however, the numerical error makes $|A(0, \chi) - B(0, \chi)|$ (and thus the temperature) deviate appreciably from a constant value. In fact, the variations become larger the larger the charge q, whereas in principle the equations should guarantee a constant value of the temperature. It is thus not surprising to see the numerical integration fail to converge for some critical value of the charge.

On the other hand, with increasing q, the supposed Hawking temperature of the configurations decreases, and configurations with appropriately large values of q would be expected to correspond to near-extremal solutions. Indeed, this reasoning suggests that, similar to GR, extremal solutions might exist, which possess a maximal value of the electric charge for a given event horizon radius, and whose temperature would be zero. However, the study of black holes which are extremal or close to extremality is a difficult numerical problem already for situations, where the existence of solutions is not controversial. Consequently, the existence of *extremal* braneworld black holes in the RS model is an open problem, which we cannot attack within our current numerical scheme. However, we will address the problem from a different direction in the next section.

3. The interpretation of the results

We think that the interpretation of our results can only be analogous to the interpretation proposed by

[10]We have considered charged configurations only in $d = 5$ dimensions.

Yoshino [9]. In particular, we would like to consider the following possibilities:

First, one might suspect that our approach and/or the numerical methods are wrong. However, similar methods[11] were used in the past to solve a variety of problems, see e.g. [22,24,25]. Moreover, we have extensively tested these numerical routines to recover numerous exact solutions in GR and field theory. At the same time, some of the new solutions derived by using the code FIDISOL/CADSOL were rederived subsequently by other groups with different numerical methods. Therefore we think that this hypothesis can be safely excluded.

The second possibility would be that static solutions exist, but that they are very hard to find, forming isolated ''islands'' in the parameter space. Moreover, these islands would be disconnected from the $L = 0$ Schwarzschild black hole used as an initial guess in the numerical attempts to construct such solutions.[12] In this setup, the numerical results found would be numerical artifacts, since the true solutions would require a starting profile different from the Schwarzschild black hole. However, we consider this possibility as counterintuitive and unlikely.

In our opinion, the most likely scenario is that there are no static solutions of the bulk Einstein equations (2.11), (2.12), and (2.13) with the boundary conditions (2.20), (2.22), and (2.23). Moreover, in agreement with the conjecture put forward by Emparan *et al.* [11] and Tanaka [12], all nonextremal black holes on the brane would be dynamical objects. If this were indeed the case, then the numerical results could be interpreted as follows: what we have found should correspond to static approximations of some yet unknown time-dependent configurations. The full solutions for black holes on the brane would be dynamical, quantum corrected, evaporating black holes; thus also the bulk solutions would depend on time. The systematic occurrence of the observed unnatural behavior of the metric functions close to the AdS horizon would be the result of an inappropriate static metric ansatz. For black holes with sizes small compared to the AdS length scale, the pathological behavior at infinity would not be seen due to the lack of numerical accuracy. In other words, for small values of $|\Lambda|$, the hyperbolic character of the equations would not become manifest, and the solver would fail to see the quantum corrections. However, as the value of $L = r_0/\ell$ increases, the neglected dynamical terms would destabilize the numerics.[13] This interpretation should hold for both vacuum and charged configurations.

III. EXTREMAL SOLUTIONS: THE NEAR-HORIZON GEOMETRY

A. The problem

The discussions in the previous section concern the case of nonextremal static black holes possessing a *nonzero* Hawking temperature. However, these findings cannot be used to argue against the existence of static extremal configurations. In contrast, static extremal configurations would have zero temperature and therefore would not Hawking radiate. Thus the arguments put forward by Emparan *et al.* [11] and Tanaka [12] against the existence of static black holes on the brane would be circumvented. From this point of view, arbitrarily large extremal black holes might indeed exist on the brane.

In principle, the metric ansatz (2.7) could still be used in an attempt to numerically construct extremal black holes, after replacing the background function F by $F(r) = (1 - (r_0/r)^{d-3})^2$. (Then the bulk metric would still depend on the coordinates r, χ.) However, the numerical construction of extremal black holes is a highly nontrivial task.[14] Therefore we do not attempt here to construct such bulk configurations numerically. Instead, in the following we only address a simplified problem and concentrate on the near-horizon region of ''potential'' extremal black holes.

Such a restricted study may well provide hints on the properties of the full black hole solutions without solving for the full metric.[15] However, we would like to emphasize that this study could only allow us to rule out possible full black hole solutions, while it cannot prove their existence, since for a given near-horizon geometry there need not be a corresponding full black hole solution.

Let us start by recalling that in GR an extremal RN solution in D dimensions (where later $D = d - 1$) has a near-horizon geometry $\mathrm{AdS}_2 \times S^{D-2}$, which is also a solution of the equations of motion. For a Lagrangian density $L = R - F^2$, the corresponding near-horizon line element reads

[11] In particular, the treatment of the behavior of the metric functions on the axis $\chi = 0$ and at infinity has been similar to that used in this work.

[12] Such examples are known for numerical solutions in field theory, the case of vortons (which are $d = 4$ flat space toroidal solitons somewhat analogous to $d = 5$ black rings) being perhaps the most notorious. There several disconnected branches of numerical solutions are known to exist, which do not possess a static limit [25,26].

[13] We note that the observed oscillatory behavior of the configurations is not predicted by perturbation theory (see [7] and references therein). However, we suspect that this is a deficiency of the perturbation theory. A somewhat similar situation is encountered in Einstein gravity coupled to non-Abelian matter fields. There perturbation theory predicted the existence of $d = 4$ rotating Einstein-Yang-Mills solitons [27]. Such configurations were, however, ruled out by nonperturbative arguments.

[14] In fact, we are not aware of any successful numerical construction of extremal black holes, obtained as solutions of second order partial differential equations.

[15] Such an approach has been used recently to investigate properties of higher dimensional extremal black holes with a nonspherical horizon topology, see e.g. [28].

$$ds^2 = L^2_{1(\mathrm{GR})} d\Sigma_2^2 + L^2_{2(\mathrm{GR})} d\Omega^2_{D-2}, \tag{3.1}$$

where

$$L^2_{1(\mathrm{GR})} = \frac{2(D-3)}{D-2} Q^2, \quad L^2_{2(\mathrm{GR})} = \frac{2(D-3)^3}{D-2} Q^2, \tag{3.2}$$

$d\Sigma_2^2 = dx^2/x^2 - x^2 dt^2$ is the line element of the two-dimensional AdS space, and the gauge field is $F_{xt} = Q$. [Note that the electric charge $\mathcal{Q}$ of the bulk RN black holes is $\mathcal{Q} = Q L^{D-2}_{2(\mathrm{GR})}/L^2_{1(\mathrm{GR})}$ (up to a volume factor).] The entropy of this solution is

$$S_{D(\mathrm{GR})} = \frac{V_D}{4G_D} L^{D-2}_{2(\mathrm{GR})}. \tag{3.3}$$

Turning now to black holes on the brane, we expect that the near-horizon geometry of static extremal black holes on the brane in the RS model will, analogously, have a near-horizon geometry $\mathrm{AdS}_2 \times S^{d-3}$ (where AdS_2 and S^{d-3} have constant radii), which should then be the induced metric on the brane. Thus we assume that this metric has a form similar to Eq. (3.1), with, in general, different values for the constant coefficients, but recovering Eqs. (3.2) and (3.3) in a certain limit.

These considerations correspond in fact to the approach of Kaus and Reall [19] used to study $d = 5$ extremal black holes, charged with respect to a Maxwell field on the brane. Kaus and Reall [19] found that the GR results are recovered for large black holes. (We further note that Suzuki *et al.* [29] examined the case of extremal black holes in a braneworld with a cosmological constant.)

B. The bulk: Equations and asymptotics

The considerations above lead us to propose the following line element for the near-horizon limit of an extremal bulk black hole[16],

$$ds^2 = \frac{d\xi^2}{f(\xi)} + a(\xi) d\Sigma_2^2 + \xi^2 d\Omega^2_{d-3}, \tag{3.4}$$

containing two metric functions $a(\xi)$ and $f(\xi)$. Here the coordinate $\xi \geq 0$ is the coordinate normal to the brane, and the brane is located at some $\xi_0 > 0$. Thus the coordinate ξ is proportional to $\sin\chi$ in the bulk parametrization Eq. (2.7).[17]

The functions $a(\xi)$ and $f(\xi)$ are solutions of the differential equations

$$\begin{aligned} &a'' - \frac{a'^2}{a^2} + \frac{(d-5)(d-4)}{2\xi^2}\left(1 - \frac{1}{f}\right) + \frac{(d-4)af'}{2\xi f} \\ &\quad + \frac{(d-4)a'}{\xi} + \frac{a'f'}{2f} + \frac{1}{f} + \frac{\Lambda a}{f} = 0, \\ &f' + \frac{4\Lambda\xi}{d-2} + \frac{2(d-4)}{\xi}(f-1) + \frac{2fa'}{a} = 0, \end{aligned} \tag{3.5}$$

together with the constraint equation

$$\begin{aligned} &a'^2 + \frac{2(d-3)(d-4)a^2}{\xi^2}\left(1 - \frac{1}{f}\right) + \frac{4a(1+\Lambda a)}{f} \\ &\quad + \frac{4(d-3)aa'}{\xi} = 0. \end{aligned} \tag{3.6}$$

These equations have the following exact solutions:

$$f(\xi) = 1 + \frac{\xi^2}{\ell^2}, \qquad a(\xi) = \xi^2 + \ell^2, \tag{3.7}$$

which correspond to AdS_d in coordinates adapted to a foliation by $\mathrm{AdS}_2 \times S^{d-2}$ hypersurfaces, and

$$f(\xi) = 1 + \frac{d-1}{d-3}\frac{\xi^2}{\ell^2}, \qquad a(\xi) = \frac{\ell^2}{d-1}, \tag{3.8}$$

which corresponds to $\mathrm{AdS}_2 \times H^{d-2}$.

For the general solutions of these equations smoothness at $\xi = 0$ requires that $a(\xi)$ and $f(\xi)$ possess a Taylor series expansion there, consisting of even powers of ξ only, with $a(0) > 0$ and $f(0) = 1$. To order ξ^4, the small ξ expansion reads

$$\begin{aligned} a(\xi) &= a_0 - \frac{d-2+2a_0\Lambda}{(d-2)^2}\xi^2 \\ &\quad + \frac{(d-2+2a_0\Lambda)((d-1)(d-2)+2a_0\Lambda)}{a_0(d-2)^4(d-3)d}\xi^4 + \cdots, \\ f(\xi) &= 1 + \frac{2(d-2-a_0(d-4)\Lambda)}{a_0(d-2)^2(d-3)}\xi^2 \\ &\quad + \frac{2(d-2+2a_0\Lambda)((d-1)(d-2)+2a_0\Lambda)}{a_0^2(d-2)^4(d-3)d}\xi^4 + \cdots. \end{aligned} \tag{3.9}$$

One can also construct an approximate solution for large values of the ratio ξ/ℓ [although we shall see that configurations with this asymptotics exist for a restricted set of initial data, $a(0) > \ell^2/(d-1)$ only], which is useful in our analytical study of large black holes. For even d, this solution reads

[16]We employed a similar metric ansatz and the same numerical methods in our previous studies [30,31] of asymptotically AdS solitons with a nonstandard asymptotic structure.

[17]The coordinate r in Eq. (2.7) becomes the coordinate x in the AdS_2 parametrization $d\Sigma_2^2 = dx^2/x^2 - x^2 dt^2$ after taking the near-horizon limit.

$$a(\xi)=U\ell^2\left(\frac{\xi^2}{\ell^2}+\sum_{k=0}^{(d-4)/2}a_k\left(\frac{\ell}{\xi}\right)^{2k}-M\left(\frac{\ell}{\xi}\right)^{d-3}\right)+O(1/\xi^{d-2}),$$
$$f(\xi)=\frac{\xi^2}{\ell^2}+\sum_{k=0}^{(d-4)/2}f_k\left(\frac{\ell}{\xi}\right)^{2k}-2M\left(\frac{\ell}{\xi}\right)^{d-3}+O(1/\xi^{d-2}), \tag{3.10}$$

where the parameter U corresponds to the asymptotic ratio of the radius of AdS_2 to that of S^{d-3}. Also, a_k and f_k are constants depending on the spacetime dimension d and U only. Specifically, one finds

$$a_0=\frac{1+(d-4)U}{U(d-3)},\qquad a_1=-\frac{(d-4)(1-U)(1+(d-4)U)}{(d-2)(d-3)^2(d-5)U^2},$$
$$a_2=\frac{(d-4)(1-U)(1+(d-4)U)(2(d-5)d-4+(d-4)(26+(3d-23)d)U)}{3(d-2)^2(d-3)^3(d-5)(d-7)U^3}, \tag{3.11}$$

and

$$f_0=\frac{2+(d-1)(d-4)U}{U(d-2)(d-3)},\qquad f_1=-\frac{2(d-4)(1-U)(1+(d-4)U)}{(d-2)(d-3)^2(d-5)U^2},$$
$$f_2=\frac{2(d-4)(1-U)(1+(d-4)U)(d(d-7)+8+(d-4)(11+(d-8)d)U)}{(d-2)^2(d-3)^3(d-5)(d-7)U^3}, \tag{3.12}$$

their expressions becoming more complicated for higher order k, without exhibiting a general pattern. The corresponding expansion for odd values of the spacetime dimension is more complicated, with $\log(\xi/\ell)$ terms in the asymptotic expression

$$a(\xi)=U\left(\frac{\xi^2}{\ell^2}+\sum_{k=0}^{(d-5)/2}a_k\left(\frac{\ell}{\xi}\right)^{2k}+q\log\left(\frac{\ell}{\xi}\right)\left(\frac{\ell}{\xi}\right)^{d-3}+\left(-M+\beta\right)\left(\frac{\ell}{\xi}\right)^{d-3}\right)+O\left(\frac{\log\xi}{\xi^{d-1}}\right),$$
$$f(\xi)=\frac{\xi^2}{\ell^2}+\sum_{k=0}^{(d-5)/2}f_k\left(\frac{\ell}{\xi}\right)^{2k}+2q\log\left(\frac{\ell}{\xi}\right)\left(\frac{\ell}{\xi}\right)^{d-3}-2M\left(\frac{\ell}{\xi}\right)^{d-3}+O\left(\frac{\log\xi}{\xi^{d-1}}\right), \tag{3.13}$$

where a_k and f_k are still given by Eqs. (3.11) and (3.12), while q and β are two new constants depending on ℓ and d that can be expressed in a compact form as

$$\beta=0\delta_{5,d}-\frac{3(1-U)^2(1+3U)}{3200U^3}\delta_{7,d}+\frac{25(1-U)^2(1+5U)(157+725U)}{42674688}\delta_{9,d}+\cdots,$$
$$q=\frac{1-U^2}{12U^2}\delta_{5,d}-\frac{3(1-U)(1+3U)(2+3U)}{800U^3}\delta_{7,d}+\frac{5(1-U)(1+5U)(171+1100U+1375U^2)}{1778112U^4}\delta_{9,d}+\cdots. \tag{3.14}$$

The parameter M in Eqs. (3.10) and (3.13) is a constant that can be fixed by numerical calculations, but whose value is not of interest in the present context.

We remark, however, that these bulk solutions are interesting in themselves, since they provide gravitational duals for some conformal field theories (CFTs) in a fixed $AdS_2\times S^{d-2}$ background given by

$$ds^2=\ell^2(U^2d\Sigma_2^2+d\Omega_{d-3}^2). \tag{3.15}$$

These configurations have a well-defined mass and action which can be computed by using the boundary counterterm prescription of Balasubramanian and Kraus [32]. [In fact, both the mass and action are essentially fixed by the parameter M in the asymptotic expansion, Eqs. (3.10) and (3.13).] The stress tensor of the dual CFT can also be calculated by the method of Myers [33]. A detailed study of these aspects will be presented elsewhere in a more general context.

C. The brane

We now assume that the brane is located at $\xi=\xi_0$, and, following the RS construction, we keep the region $0\le\xi\le\xi_0$ of the bulk. The induced metric on the brane is a product of AdS_2 and S^{d-2}, with

$$d\sigma^2=L_1^2d\Sigma_2^2+L_2^2d\Omega_{d-3}^2, \tag{3.16}$$

where

$$L_1=\sqrt{a(\xi_0)},\qquad L_2=\xi_0. \tag{3.17}$$

Similar to the case of Einstein-Maxwell gravity discussed above, we shall take a purely electric field with $F_{xt}=Q$.

(Note that, similar to the GR case, the electric charge of the full solution on the brane would be only proportional to Q.)

The Israel junction conditions on the brane, Eq. (2.5), yield the relation

$$\frac{a'(\xi_0)}{a(\xi_0)} = \frac{2}{3}\left(\frac{2(d-2)}{\ell\sqrt{f(\xi_0)}} - \frac{2d-7}{\xi_0}\right), \tag{3.18}$$

together with

$$Q^2 = \frac{1}{3}(d-2)(d-3)\frac{a^2(\xi_0)}{\ell\xi_0}\left(\sqrt{f(\xi_0)} - \frac{\xi_0}{\ell}\right). \tag{3.19}$$

Then the constraint equation (3.6) implies that

$$\frac{1}{L_1^2} - \frac{(d-3)(d-4)}{2L_2^2} = \frac{Q^2}{L_1^4}\left(\frac{d-5}{d-3} + \frac{7d-23}{2(d-2)(d-3)^2}\frac{\ell^2 Q^2}{L_1^4}\right), \tag{3.20}$$

(which has been used to test the accuracy of the numerical results). Moreover, this relation implies $L_2 > L_1$; thus the S^{d-3} radius is always greater than the AdS_2 radius.

The entropy of the bulk solution is taken to be one-quarter of the event horizon area (note the factor of 2 which originates from the Z_2 symmetry of the problem)

$$S_d = 2\frac{V_{d-3}}{4G_d}\int_0^{\xi_0} d\xi \frac{\xi^{d-3}}{\sqrt{f(\xi)}}. \tag{3.21}$$

D. The solutions

1. General results

We have solved the bulk equations (3.5) by imposing the initial conditions (3.9) together with the boundary conditions on the brane (3.18) and (3.19) for all dimensions between 5 and 9. Thus such solutions are likely to exist for any higher dimension d. Different from the strategy employed in Sec. II, when trying to solve for the full configurations, we have here fixed the AdS length scale $\ell = 1$ and varied instead the position of the brane, i.e., the size of the black hole as given by the parameter L_2, Eq. (3.17).

The near-horizon region of the extremal black holes has then been constructed in several steps as follows. First, we have solved numerically the Einstein equations (3.5) by employing a standard ordinary differential equation solver. In particular, for a given value a_0, we have evaluated the initial conditions (3.9) at $\xi = 10^{-6}$ and allowed for a global tolerance of 10^{-12}, when integrating toward large values of ξ. (We note that we have not encountered any problems in the numerical integration of the configurations in this section.) Given such a solution of the bulk Einstein equations, in the second step we have used the junction condition (3.18) to evaluate the position ξ_0 of the brane. In the final step, the corresponding value of the charge parameter Q has been obtained from condition (3.19).

Our results indicate the existence of a single parameter family of solutions of the full problem (i.e., bulk plus brane), conveniently labeled by the value $a(0)$. The basic features of these solutions are independent of the dimension d. First, for $0 < a(0) \leq \ell^2/(d-1)$, the bulk solutions do not approach the asymptotic form (3.10) and (3.13). Instead, the function $a(\xi)$ decreases monotonically and vanishes at some finite radius $\xi_{\max}$, which is a curvature singularity, as seen e.g. by evaluating the Kretschmann scalar. However, such configurations are also relevant in the present context, since the junction condition (3.18) possesses a solution with $\xi_0 < \xi_{\max}$. (Thus the singularity is outside the physical manifold.)

Solutions of the Einstein equations which for sufficiently large values of ξ approach the asymptotic forms (3.10) and (3.13) are present for $a(0) > \ell^2/(d-1)$. In this case, there occurs a maximal value of $a(0)$ as well, since the junction condition (3.18) can be satisfied only for $a(0) < a_c$, where the critical value a_c depends on the dimension. While $a_c = 1$ for $d = 5$, approximate values for a_c are 0.43, 0.28, and 0.21 for $d = 6$, 7, and 8, respectively. Also, the position of the brane as given by ξ_0 is a monotonic function of $a(0)$, with both ξ_0/ℓ and Q diverging as $a(0) \to a_c$, while the parameter U stays finite in this limit.

The functions $a(\xi)$ and $f(\xi)$ of $d = 6$ bulk solutions are exhibited in Fig. 3 for several values of the initial parameter $a(0)$. Note that the picture here is generic (as seen e.g. by comparing with the figures obtained by Kaus and Reall [19] for $d = 5$). The exact solution (3.8) clearly separates the two different types of configurations.

In Fig. 4 we exhibit the parameters L_1, L_2, and S_d for $d = 6$ and 7 solutions, normalized with respect to the corresponding Einstein-Maxwell results, Eqs. (3.2) and (3.3) with $D = d - 1$. For any d, the parameters L_1, L_2, and S_d vanish as $Q \to 0$. However, both $L_1/L_{1(\mathrm{GR})}$ and $L_2/L_{2(\mathrm{GR})}$ diverge in this limit; at the same time, the ratio S_d/S_{d-1} approaches a constant nonzero value (e.g. $S_d/S_{d-1} \simeq 0.14$, 0.078, and 0.095 for $d = 5$, 6, and 7, respectively). Moreover, for sufficiently large values of Q, the GR results are recovered.

For $d = 5$, we have the choice to consider an electric or a magnetic charge on the brane. However, similar to the case of Einstein-Maxwell gravity, one can show that the properties of the solution are the same in both cases and the electric-magnetic U(1) duality still holds.[18] Our numerical results for $d = 5$ are in good agreement with those in [19]. (We note, however, that in [19] a different parametrization of the metric was employed.)

2. The large black holes limit

The observation that ξ_0/ℓ diverges as $a(0) \to a_c$ implies that one can use the asymptotic expressions (3.10) and

[18]We thank H. Reall for a correction on this issue.

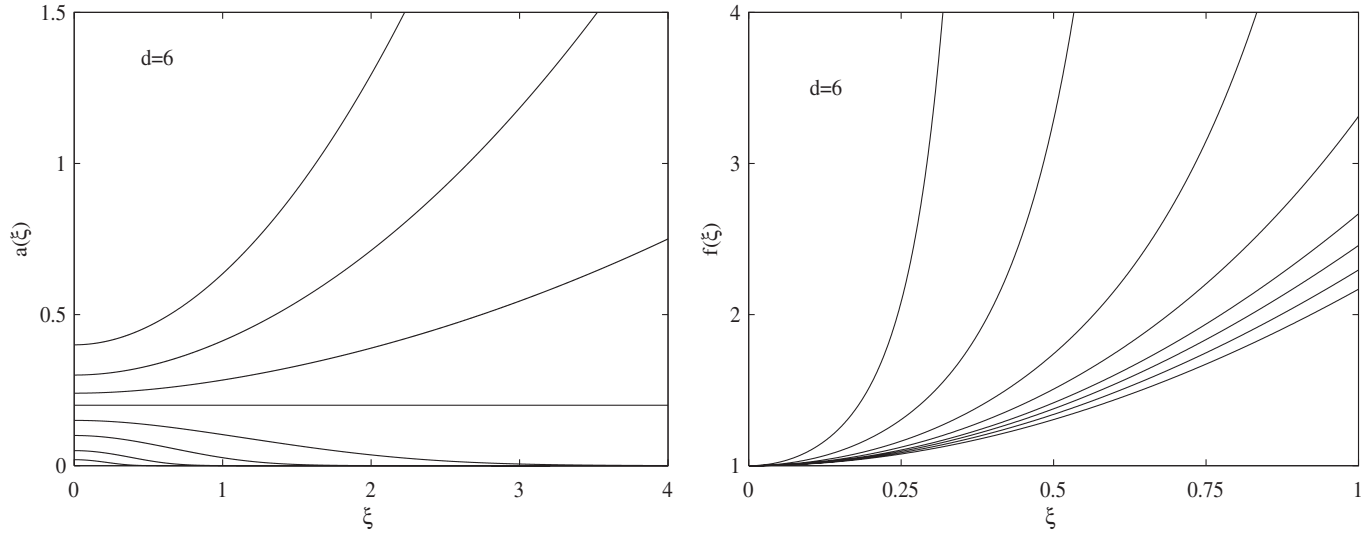

FIG. 3. The functions $a(\xi)$ and $f(\xi)$ are shown for $d = 6$ and $\ell = 1$. The initial parameter assumes the values $a(0) = 0.4$, 0.3, 0.24, 0.2, 0.15, 0.1, 0.05, and 0.02 from top to bottom (left figure) and from left to right (right figure).

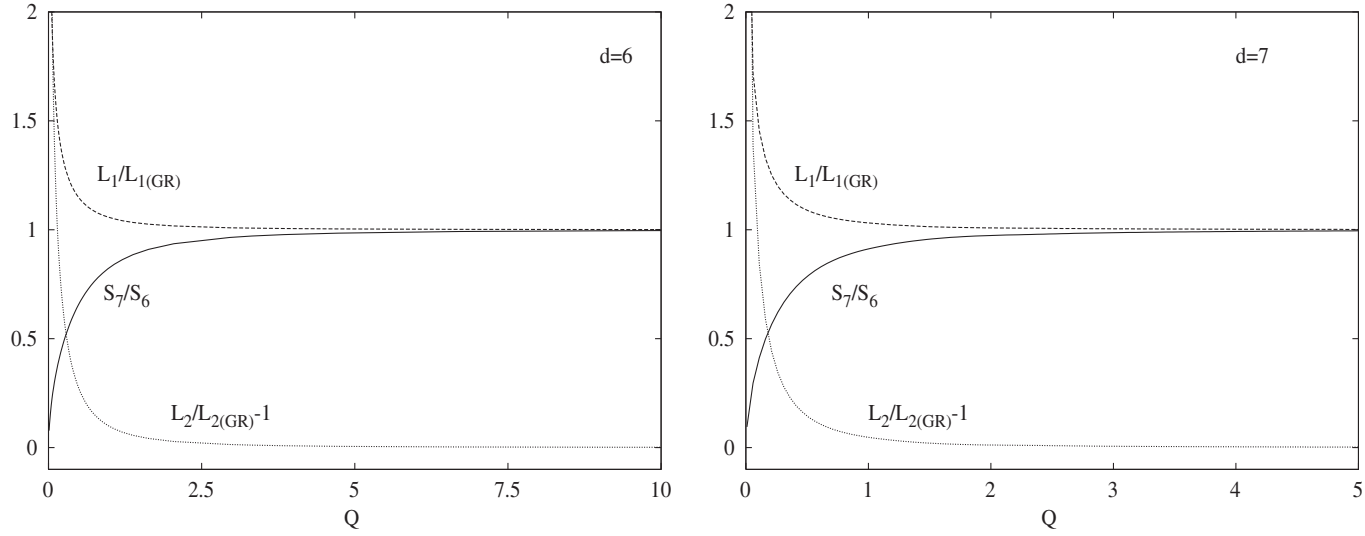

FIG. 4. The ratios S_d/S_{d-1}, $L_1/L_{1(\mathrm{GR})}$, and $L_2/L_{2(\mathrm{GR})}$ (shifted by -1) are shown for $d = 6$ and 7 with $\ell = 1$.

(3.13) to derive a number of simple analytic results for large black holes, and thus to understand the large-Q behavior, demonstrated in Fig. 4. Following Kaus and Reall [19], one starts by assuming an asymptotic expression for the parameter U [which enters the large-ξ expansion (3.10) and (3.13)] in terms of a power series in $\epsilon = \ell/\xi_0$. Then the first junction condition (3.18) implies that

$$U = \frac{1}{(d-4)^2} - \frac{(d-3)(4d-11)}{4(d-2)(d-4)^2}\epsilon^2 + \cdots. \tag{3.22}$$

This shows that the metric function $a(\xi_0)$ (i.e., the size of the AdS_2 part of the brane metric) has the following approximate form on the brane:

$$a = L_1^2 = \frac{1}{(d-4)^2}\frac{\ell^2}{\epsilon^2} - \frac{(d-1)\ell^2}{4(d-2)(d-4)^2} + \cdots. \tag{3.23}$$

The second junction condition (3.18) gives for the charge parameter the expression

$$Q^2 = \frac{d-3}{2(d-4)^3}\frac{\ell^2}{\epsilon^2} - \frac{(d-3)(7d-18)}{8(d-2)(d-4)^3}\ell^2 + \cdots. \tag{3.24}$$

Inversion of Eqs. (3.22) and (3.23) yields ϵ as a function of Q^2. One obtains

$$L_1^2 = \frac{2(d-4)}{(d-3)}Q^2 + \frac{6d-19}{4(d-2)(d-4)^2}\ell^2 + \cdots, \tag{3.25}$$

$$L_2^2 = \frac{2(d-4)^3}{(d-3)} Q^2 + \frac{7d-18}{4(d-2)} \ell^2 + \cdots, \tag{3.26}$$

where comparison with (3.1) (with $D = d - 1$) shows agreement with GR in the limit of large Q/ℓ. (Note that the leading order corrections are strictly positive.)

The same holds also for the entropy of these solutions, which, in $d > 5$ dimensions, is given by

$$S_d = 2\frac{V_{d-3}}{4G_d} \frac{\ell}{(d-3)} \xi_0^{d-3} \left(1 - \frac{3(d-3)(d-4)}{2(d-2)(d-5)} \frac{\ell^2}{\xi_0^2}\right) + \cdots. \tag{3.27}$$

The first term here corresponds to the entropy of an extremal RN black hole in $d - 1$ dimensions. [Recall that $G_d = [2\ell/(d-3)]G_{d-1}$.] With the help of relation (3.24), one can reexpress S_d as a function of the charge parameter Q. As seen from the large-Q region of Fig. 4, the analytical and numerical results are in excellent agreement.

For $d = 5$, the leading order correction for the entropy as a function of Q contains a log term, which is absent in other dimensions. The corresponding relations are given in [19], together with some relevant plots.[19]

IV. FURTHER REMARKS

In this work we have addressed the issue of black hole solutions in the RS infinite braneworld scenario, allowing the black holes to carry electric charge on the brane. In the first part of the paper we have considered vacuum black holes and nonextremal charged black holes on the brane. Employing a different numerical technique by solving the set of elliptic partial differential equations in the full bulk, ranging from the brane to the AdS horizon, we have obtained results that fully support the claim by Yoshino [9] for the nonexistence of static vacuum black holes on an asymptotically flat brane in the RS infinite braneworld model. This conclusion does not change when (nonextremal) solutions are considered, which are charged with respect to a Maxwell field living on the brane. Although ''approximate'' solutions appear to exist for sufficiently small brane tension, these configurations are very likely only numerical artifacts.

One should emphasize that, of course, the numerical results cannot be used to prove the nonexistence of static black hole solutions on the brane. To clarify the issue of the existence of black holes on the brane one would thus need to either find a full analytic solution or, alternatively, to provide a rigorous theoretical argument for the absence of such black hole solutions. Lacking both, however, we think that a natural interpretation of our and previous numerical results is provided by the conjecture that nonextremal braneworld black holes would necessarily be time dependent [11,12].

The situation is different for extremal black holes, since the conjecture put forward by Emparan *et al.* [11] and Tanaka [12] does not forbid the existence of static extremal black holes. Thus, in principle, the presence of a second global charge, apart from the mass, could allow for the existence of extremal black holes also in a braneworld context. While the numerical construction of localized extremal black holes still represents a numerical challenge to be met, we here have considered the less ambitious task of constructing only the near-horizon geometry of extremal solutions with a Maxwell field on the brane. In particular, we have found that the GR predictions in $d - 1$ dimensions are reproduced for extremal black holes which are sufficiently large as compared to the AdS scale.

One should mention, though, that finding local solutions in the vicinity of the horizon does not guarantee the existence of the corresponding global solutions. (Chen *et al.* [34], for instance, give an example where the physically relevant global solutions are absent despite the presence of a closed form near-horizon solution.) In our opinion, any progress in this direction would require the development of a consistent numerical scheme capable to achieve the explicit construction of the bulk extremal black holes.

However, another physically interesting situation to consider in the context of the RS infinite braneworld model concerns the case of static localized solitons on the brane. With no event horizon present, solitons do not possess intrinsic thermodynamical properties. Thus the conjecture of Emparan *et al.* [11] and Tanaka [12] has no obvious bearing on the existence of solitons on the brane.

Let us thus consider as the simplest example of (possible) solitons on the brane in the RS model, the case of braneworld Q-balls based on the matter field Lagrange density

$$\mathcal{L}_Q = \partial_\mu \Phi^* \partial^\mu \Phi + U(|\Phi|). \tag{4.1}$$

The matter field in this case is a complex scalar field Φ with a harmonic time dependence and a nonrenormalizable self-interaction described by the potential $U(|\Phi|)$. The flat spacetime solutions of this theory were considered for the first time by Coleman [35], while their Einstein gravity generalizations were discussed in [36–38]. These gravitating nontopological solitons describe localized particlelike objects with finite energy.

We have attempted to construct $d = 5$ spherically symmetric gravitating Q-balls in the RS model, where the scalar field is confined to the brane and described by the simple ansatz

$$\Phi = f(r) e^{-iwt}, \tag{4.2}$$

[19]For $d = 5$, the electric charge is $\mathcal{Q} = (L_2^2/L_1^2)Q$.

where we have followed a basically similar approach for these gravitating Q-balls as for the static black hole solutions. In particular, we have tried to solve the bulk Einstein equations numerically for the metric ansatz (2.7) with $r_0 = 0$, where the boundary conditions at $r = 0$, $r = \infty$, and $\chi = 0$ are still given by (2.20), (2.21), and (2.22) (with $r_0 = 0$) and (2.5), respectively, and where the energy-momentum tensor is given by

$$t_{\mu\nu} = \partial_\mu \Phi^* \partial_\nu \Phi + \partial_\nu \Phi^* \partial_\mu \Phi - g_{\mu\nu} \mathcal{L}_Q. \tag{4.3}$$

However, unexpectedly, our attempts to construct gravitating Q-balls on the brane have not been successful. As in our attempts to construct static black hole solutions on the brane, we have failed here to obtain reliable numerical gravitating Q-ball solutions on the brane. Interestingly, the reason for the numerical inaccuracy of the configurations and the lack of the numerical convergence again resides in the unnatural far field behavior of the metric functions close to the AdS horizon. In fact, this unnatural far field behavior is completely analogous to one observed for the configurations supposed to describe static black holes.

Clearly, this behavior is hard to understand, since there is no clear *a priori* reason for solitons *not* to exist on the brane. However, if we interpret our results for the static (nonextremal) black hole solutions as implying that there are no such solutions on the brane (satisfying the given set of equations and boundary conditions), we must, consistently, draw the same conclusion for the gravitating Q-ball solutions. While it might be interesting to attempt the construction of other types of solitons on the brane, the present results strongly discourage such a construction, since the same problems in the vicinity of the AdS horizon are likely to arise.

How do we then judge the issue of black holes and regular solutions on the brane? There are still the positive results from the near-horizon black hole solutions in the extremal case, but these extremal near-horizon solutions avoid the problematic region in the vicinity of the AdS horizon. Thus a full calculation of extremal solutions is clearly called for, where one attempts to smoothly extend the near-horizon geometry of the extremal solutions into the asymptotic region, in spite of the tremendous numerical challenge. The final outcome might, however, be that one is led to conclude that there are no extremal black hole solutions on the brane, either.

ACKNOWLEDGMENTS

We thank H. Reall for important comments on the first version of this work. E. R. would like to thank M. Volkov for useful discussions. B. K. gratefully acknowledges support by the DFG. The work of E. R. was supported by the Alexander von Humboldt Foundation and the Science Foundation Ireland (SFI) Project No. RFP07-330PHY.

APPENDIX: THE NUMERICAL METHOD

The set of three coupled nonlinear elliptic partial differential equations for the functions A, B, and C has been solved numerically for the (ρ, χ) coordinate system introduced in Sec. II A 1, subject to the boundary conditions (2.20), (2.21), (2.22), and (2.23).

The first step has been to introduce a new radial variable $x = \rho/(1 + \rho)$ which maps the semi-infinite region $[0, \infty)$ to the finite region $[0, 1]$. This involves the following substitutions in the differential equations:

$$\rho u_{,\rho} \to (1 - x) f_{,x}, \quad \rho^2 u_{,\rho\rho} \to (1 - x)^2 u_{,xx} - 2(1 - x) u_{,x}, \tag{A1}$$

where u denotes any of the unknown functions A, B, or C.

Next the equations for these functions are discretized on a nonequidistant grid in x and χ. Here we have considered various grid choices, the number of grid points ranging between 180×30 and 80×70. The grid covers the integration region $0 \le x \le 1$ and $0 \le \chi \le \pi/2$. Typically, the mesh in the x direction has been denser in the near-horizon region ($x = 0$) and for values of x close to the AdS horizon. Most of the χ meshes employed have been equidistant.

All numerical calculations have been performed by using the programs FIDISOL/CADSOL [23]. Here we shall briefly review its basic aspects. The code requests the system of nonlinear partial differential equations in the form

$$P(x, y, u, u_x, u_y, u_{xy}, u_{xx}, u_{yy}) = 0, \tag{A2}$$

subject to a set of boundary conditions on a rectangular domain. (For convenience, we have used the notation $\chi \equiv y$.) Besides the set of equations, FIDISOL/CADSOL requires the boundary conditions, the Jacobian matrices for the equations, and the boundary conditions, as well as some initial guess for the functions. The Jacobian matrices are generated by simple differentiation of each equation P with respect to u, u_x, u_y, u_{xy}, u_{xx}, and u_{yy}.

FIDISOL/CADSOL uses a Newton-Raphson method. The numerical procedure works as follows: for an approximate solution $u^{(1)}$, $P(u^{(1)})$ does not vanish. The next step is then to consider an improved solution

$$u^{(2)} = u^{(1)} + w \Delta u, \tag{A3}$$

supposing that $P(u^{(1)} + w\Delta u) = 0$ (with w a relaxation factor, which is usually chosen as $w = 1$). The expansion in the small parameter Δu gives to first order

$$0 = P(u^{(1)} + \Delta u) \approx P(u^{(1)}) + \frac{\partial P}{\partial u}(u^{(1)}) \Delta u + \cdots. \tag{A4}$$

This equation is then used to determine the correction $\Delta u^{(1)} = \Delta u$. Repeating these calculations iteratively ($u^{(3)} = u^{(2)} + \Delta u$, etc.), the approximate solutions will converge, provided the initial guess is close enough to the true solution. In each step, a linear system of equations

is solved, and the residual $\|P(u^{(i)})\|$ decreases by a factor of approximately 10–20. The iteration stops after i steps, when the Newton residual $P(u^{(i)})$ is smaller than a prescribed tolerance. Clearly, it is essential to have a good first guess, to start the iteration procedure.

The package FIDISOL/CADSOL provides also error estimates for each function, which allows one to judge the quality of the computed solution. The errors are computed on the ''consistency level,'' namely, the discretized Newton residual, and as discretization error terms in x, y directions. The discretization error is estimated through the difference of difference quotients. For example, in (A4), the derivative of the solution u and of the correction function Δu are discretized by a difference method with arbitrary consistency orders. Derivatives are replaced, for example, in the form $u_{xx} \Leftarrow u_{xx,d} + d_{xx}$, $\Delta u_{xx} \Leftarrow \Delta u_{xx,d}$, where the index d means ''discretized.'' d_{xx} is the estimate for the discretization (or truncation) error of u_{xx}, defined as $d_{xx} = u_{xx,d,\mathrm{next}} - u_{xx,d}$, where the index ''next'' denotes the next higher member of the family of nonequidistant backward difference formulas. The discretized Newton residual decreases with the number of Newton-Raphson iterations, while the discretization error terms depend on the grid size and the used consistency order, i.e. on the order of the discretization of derivatives (in our work, this order was 6). Furthermore, the error terms are used for the determination of stopping criteria for the Newton-Raphson method. Further details on the numerical method and explicit examples are provided in [23].

In this scheme, the input parameters are the event horizon radius r_0 and the value ℓ of the AdS length scale which form the dimensionless parameter $L = r_0/\ell$. In our approach we set $r_0 = 1$ and we start with the Schwarzschild-Tangherlini solution as an initial guess (i.e., $L = 0$ and $A = B = C = 0$). Then we increase the value of L slowly. The iterations converge, and, in principle, repeating the procedure we obtain in this way solutions for higher values of L. In some of the calculations, we interpolate the resulting configurations on points between the chosen grid points, and then use these for a new guess on a finer grid.

[1] L. Randall and R. Sundrum, Phys. Rev. Lett. **83**, 4690 (1999).
[2] P. Kanti, J. Phys. Conf. Ser. **189**, 012020 (2009).
[3] R. Emparan, G. T. Horowitz, and R. C. Myers, J. High Energy Phys. 01 (2000) 007.
[4] J. F. Plebanski and M. Demianski, Ann. Phys. (N.Y.) **98**, 98 (1976).
[5] N. Dadhich, R. Maartens, P. Papadopoulos, and V. Rezania, Phys. Lett. B **487**, 1 (2000).
[6] T. Shiromizu, K. i. Maeda, and M. Sasaki, Phys. Rev. D **62**, 024012 (2000).
[7] H. Kudoh, T. Tanaka, and T. Nakamura, Phys. Rev. D **68**, 024035 (2003).
[8] H. Kudoh, Prog. Theor. Phys. **110**, 1059 (2003).
[9] H. Yoshino, J. High Energy Phys. 01 (2009) 068.
[10] D. Karasik, C. Sahabandu, P. Suranyi, and L. C. R. Wijewardhana, Phys. Rev. D **69**, 064022 (2004); **70**, 064007 (2004).
[11] R. Emparan, A. Fabbri, and N. Kaloper, J. High Energy Phys. 08 (2002) 043.
[12] T. Tanaka, Prog. Theor. Phys. Suppl. **148**, 307 (2002).
[13] A. L. Fitzpatrick, L. Randall, and T. Wiseman, J. High Energy Phys. 11 (2006) 033.
[14] P. R. Anderson, R. Balbinot, and A. Fabbri, Phys. Rev. Lett. **94**, 061301 (2005).
[15] A. Fabbri, S. Farese, J. Navarro-Salas, G. J. Olmo, and H. Sanchis-Alepuz, Phys. Rev. D **73**, 104023 (2006).
[16] D. C. Dai and D. Stojkovic, arXiv:1004.3291.
[17] P. Kanti, I. Olasagasti, and K. Tamvakis, Phys. Rev. D **68**, 124001 (2003).
[18] A. Chamblin, H. S. Reall, H.-a. Shinkai, and T. Shiromizu, Phys. Rev. D **63**, 064015 (2001).
[19] A. Kaus and H. S. Reall, J. High Energy Phys. 05 (2009) 032.
[20] W. Israel, Nuovo Cimento B **44**, 1 (1966); **48**, 463(E) (1967).
[21] T. Wiseman, Classical Quantum Gravity **20**, 1137 (2003).
[22] B. Kleihaus, J. Kunz, and E. Radu, J. High Energy Phys. 06 (2006) 016.
[23] W. Schönauer and R. Weiß, J. Comput. Appl. Math. **27**, 279 (1989); M. Schauder, R. Weiß, and W. Schönauer, The CADSOL Program Package, Universität Karlsruhe, Interner Bericht No. 46/92, 1992.
[24] B. Kleihaus and J. Kunz, Phys. Rev. Lett. **79**, 1595 (1997); Phys. Rev. D **57**, 6138 (1998).
[25] E. Radu and M. S. Volkov, Phys. Rep. **468**, 101 (2008).
[26] R. A. Battye and P. M. Sutcliffe, Nucl. Phys. **B814**, 180 (2009); P. Grandclement, J. Comput. Phys. **229**, 3334 (2010).
[27] M. S. Volkov and N. Straumann, Phys. Rev. Lett. **79**, 1428 (1997); J. J. Van der Bij and E. Radu, Int. J. Mod. Phys. A **17**, 1477 (2002); B. Kleihaus, J. Kunz, and F. Navarro-Lerida, Phys. Rev. D **66**, 104001 (2002).
[28] P. Figueras, H. K. Kunduri, J. Lucietti, and M. Rangamani, Phys. Rev. D **78**, 044042 (2008); H. K. Kunduri and J. Lucietti, Commun. Math. Phys. **303**, 31 (2011).
[29] R. Suzuki, T. Shiromizu, and N. Tanahashi, Phys. Rev. D **82**, 085029 (2010).
[30] R. B. Mann, E. Radu, and C. Stelea, J. High Energy Phys. 09 (2006) 073.

[31] B. Kleihaus, J. Kunz, and E. Radu, J. High Energy Phys. 09 (2010) 047.
[32] V. Balasubramanian and P. Kraus, Commun. Math. Phys. **208**, 413 (1999).
[33] R. C. Myers, Phys. Rev. D **60**, 046002 (1999).
[34] C. M. Chen, D. V. Gal'tsov, N. Ohta, and D. G. Orlov, Phys. Rev. D **81**, 024002 (2010).
[35] S. R. Coleman, Nucl. Phys. **B262**, 263 (1985); **B269**, 744 (E) (1986).
[36] T. D. Lee and Y. Pang, Phys. Rep. **221**, 251 (1992).
[37] R. Friedberg, T. D. Lee, and Y. Pang, Phys. Rev. D **35**, 3658 (1987).
[38] B. Kleihaus, J. Kunz, and M. List, Phys. Rev. D **72**, 064002 (2005).